PRAMANA
— journal of
physics

© Indian Academy of Sciences

Vol. 70, No. 4
April 2008
pp. 753–758

Formation of H-atom in 2s excited state of proton-lithium and proton-sodium scattering

Y N TIWARI
Department of Physics, North-Eastern Hill University, Shillong 793 022, India
E-mail: yntiwari@gmail.com

MS received 22 November 2006; revised 4 October 2007; accepted 27 November 2007

Abstract. The differential and total cross-sections have been investigated in the formation of H-atom in the 2s excited state of proton-lithium and proton-sodium scattering by using the Coulomb projected Born (CPB) approximation in the energy range from 50 to 10,000 keV. The results thus obtained are compared with the available results and found to be in reasonable agreement.

Keywords. Total cross-section; differential cross-section; Coulomb projected Born approximation.

PACS No. 34.70+e

1. Introduction

A process in which a projectile ion captures an electron from the neutral target and turns into a bound state is known as electron capture (charge transfer, charge exchange, electron transfer). The case of electron capture is more difficult to treat than excitation or ionization. The theory of direct reactions is essentially straightforward leaving aside the technical details; most of the attention within the field of non-relativistic ion–atom collisions has been focused on electron capture. This subject hence needs broader attention. The reason for the difficulties encountered in the theoretical description, lies in the fact that electron capture is a rearrangement collision governed by two different atomic Hamiltonians, one for the target and the other for the projectile. The importance of electron processes in man-made plasma (Tokomak), controlled thermonuclear fusion, astrophysical plasmas and cometatry's atmosphere are found in different texts. Another manifestation of electron capture is seen in the radiation damage in human tissues. Within the track of the primary radiation, secondary particles such as electrons and ions are found. It is the interaction of these secondaries with biologically relevant structures such as DNA that may cause major biological damage [1–3].

Different approximate methods have been proposed by previous workers which are discussed in review articles [4–7]. The formation of H(2s) atom in the process $H^+ + Li \rightarrow H(2s) + Li^+$ has been studied only in low energy ranges. The electron capture cross-section from Li by high energy (for heavy particle collision on atoms the

ratio of the projectile velocity to the orbital electron velocity is much larger than 1) incident protons in the energy range between 200 and 10,000 keV have been investigated by Banyard and Shirtcllife [8] by using the continuum distorted wave (CDW) approximation. Basuchoudhury and Sural [9] have also studied proton-alkali atom (Na, K, Rb, Cs) collisions in the wave formulation of the impulse approximation in the energies ranging from 50 to 500 keV.

We have considered a typical electron capture reaction process capable of yielding intense energetic neutral beams of the type

$$\mathrm{H}^+ + \mathrm{A} \rightarrow \mathrm{H(2s)} + \mathrm{A}^+, \tag{1}$$

where A stands for Li and Na in their ground state. We have employed the Coulomb projected Born (CPB) approximation of Geltman [10], which is the first order high-energy approximation, to calculate the cross-section for the process (1). Our Li-atom results are in good agreement with those of Banyard and Shirtcllife. We have also compared our results with those of Ferrante *et al* [11] in Oppenheimer, Brinkman and Kramers (OBK) approximation. Na-atom results have been compared with ref. [9]. Throughout this paper atomic units have been used ($m = e = \hbar = 4\pi\varepsilon_0 = a_0 = 1$) and the total cross-sections which are expressed in units of πa_0^2 ($= 8.8 \times 10^{-17}$ cm^2) and energy in units of keV.

2. Theory

The position vectors of the atomic electron (e^-) with respect to the projectile (H^+) and the target nucleus (A^+) are denoted by $\vec{r}$ and $\vec{r}_1$ respectively. $\vec{R}$ is the position vector of the projectile with respect to the target nucleus. $\vec{R}_\mathrm{i}$ is the position vector of the projectile with respect to the CM of target nucleus and the electron and $\vec{R}_\mathrm{f}$ is the position vector of the CM of the projectile and the atomic electron with respect to the target nucleus. The differential cross-section for the process (1) from initial state i to final state f can be written as [12]

$$\frac{\mathrm{d}\sigma}{\mathrm{d}\Omega} = \frac{\mu_\mathrm{i}\mu_\mathrm{f}k_\mathrm{f}}{4\pi^2 k_\mathrm{i}}|T_\mathrm{if}^\mathrm{CPB}|^2, \tag{2}$$

where μ_i and μ_f are the reduced masses in the initial and final channels respectively. $\vec{k}_\mathrm{i}$ and $\vec{k}_\mathrm{f}$ are the wave vectors in the respective channels.

The transition matrix elements are given by

$$T_\mathrm{if}^\mathrm{CPB} = \int \phi_\mathrm{f}^*(\vec{r})\psi_\mathrm{f}^*(\vec{R}_\mathrm{f})V_\mathrm{f}\phi_\mathrm{i}(\vec{r}_1)\psi_\mathrm{i}(\vec{R}_\mathrm{i})\mathrm{d}\vec{r}_1\mathrm{d}\vec{R}_\mathrm{i}, \tag{3}$$

$$\text{where} \quad \phi_\mathrm{f}(\vec{r}) = \frac{1}{2\pi\sqrt{2\pi}}\left(1 + \beta\frac{\partial}{\partial\beta}\right)\mathrm{e}^{-\beta r}, \quad \beta = 0.5 \tag{3a}$$

$$\psi_\mathrm{f}(\vec{R}_\mathrm{f}) = \mathrm{e}^{-\pi\alpha/2}\Gamma(1 - i\alpha)_1F_1(i\alpha; 1; -ik_\mathrm{f} - i\vec{k}_\mathrm{f}\cdot\vec{R}_\mathrm{f})\mathrm{e}^{i\vec{k}_\mathrm{f}\cdot\vec{R}_\mathrm{f}} \tag{3b}$$

$$V_\mathrm{f} = -\frac{Z_T}{r_1}, \tag{3c}$$

$$\psi_\mathrm{i}(\vec{R}_\mathrm{i}) = \mathrm{e}^{i\vec{k}\cdot\vec{R}_\mathrm{i}}, \tag{3d}$$

$$\phi_{\rm i}(\vec{r}_1) = \frac{1}{2\sqrt{\pi}} \sum_{n=1}^{n=2,3} C_n \left(-\frac{\partial}{\partial S_n}\right)^{n-1} {\rm e}^{-S_n r_1}. \tag{3e}$$

$\phi_{\rm i}(\vec{r}_1)$ are the wave functions of the alkali atoms (Li and Na) in their ground state due to Simsic and Williamson, Jr [13] and have been written in the differential form to generate the various terms. For Li and Na, n varies from 1 to 2 and 1 to 3 respectively.

The values C_n and S_n are determined by the Slater's method where for Li: $C_1 = 0.39888$, $S_1 = 0.65$, $C_2 = -1.496099$, $S_2 = 2.7$ and for Na: $C_1 = 1.5628976$, $S_1 = 10.7$, $C_2 = -2.2325131$, $S_2 = 3.425$, $C_3 = 0.1429190$ and $S_3 = 0.733$.

Substituting eqs (3a)–(3e) in eq. (3), we get

$$T_{\rm if}^{\rm CPB} = -\frac{3}{4\pi\sqrt{2}} {\rm e}^{-\pi\alpha/2}\Gamma(1+i\alpha)\left(1+\beta\frac{\partial}{\partial\beta}\right)\frac{\partial}{\partial\beta}\sum C_n\left(\frac{\partial}{\partial S_n}\right)^{n-1} \times \int {\rm e}^{i(\vec{k}_{\rm i}\cdot\vec{R}_{\rm i} - \vec{k}_{\rm f}\cdot\vec{R}_{\rm f})}\, {}_1F_1(-i\alpha;1;ik_{\rm f}R_{\rm f} + i\vec{k}_{\rm f}\cdot\vec{R}_{\rm f})\frac{{\rm e}^{-\beta r}{\rm e}^{-S_n r_1}}{r r_1}{\rm d}\vec{r}_1{\rm d}\vec{R}_{\rm i} \tag{4}$$

$$T_{\rm if}^{\rm CPB} = -\frac{3}{4\pi\sqrt{2}} {\rm e}^{-\pi\alpha/2}\Gamma(1+i\alpha)\left(1+\beta\frac{\partial}{\partial\beta}\right)\frac{\partial}{\partial\beta}\sum C_n\left(\frac{\partial}{\partial S_n}\right)^{n-1} I, \tag{5}$$

where

$$I = \int {\rm e}^{i(\vec{k}_{\rm i}\cdot\vec{R}_{\rm i} - \vec{k}_{\rm f}\cdot\vec{R}_{\rm f})}\, {}_1F_1(-i\alpha;1;ik_{\rm f}R_{\rm f} + i\vec{k}_{\rm f}\cdot\vec{R}_{\rm f})\frac{{\rm e}^{-\beta r}{\rm e}^{-S_n r_1}}{r r_1}{\rm d}\vec{r}_1{\rm d}\vec{R}_{\rm i}. \tag{6}$$

Using the Fourier transform

$$\frac{{\rm e}^{-\lambda r}}{r} = \frac{1}{2\pi^2}\int \frac{{\rm e}^{i\vec{p}\cdot\vec{r}}}{(p^2+\lambda^2)}{\rm d}\vec{p} \tag{7}$$

eq. (6) takes the form

$$I = \frac{2}{\pi\mu_a^2}\int \frac{{\rm e}^{i(\mu_b\vec{k}_{\rm i} + \vec{q} - \vec{k}_{\rm f})\cdot\vec{R}_{\rm f}}\, {}_1F_1(-i\alpha;1;-ik_{\rm f}R_{\rm f} - i\vec{k}_{\rm f}\cdot\vec{R}_{\rm f})}{\left[|\vec{q} + \mu_C\vec{k}_{\rm i}|^2 + \frac{\beta^2}{\mu_a^2}\right][q^2 + S_n^2]}{\rm d}\vec{q}{\rm d}\vec{R}_{\rm f}, \tag{8}$$

where $\mu_C = (\mu_b - \frac{1}{\mu_a})$. Using the Feynman identity [14]

$$\frac{1}{ab} = \int_0^1 \frac{{\rm d}x}{[ax + b(1-x)]^2} \tag{9}$$

eq. (8) can be written as

$$I = \int\int_0^1 \frac{{\rm e}^{i[\vec{K}_s + (x-1)\vec{C}]\cdot\vec{R}_{\rm f}}}{(t_1^2 + \eta_1^2)^2}\, {}_1F_1(-i\alpha;1;ik_{\rm f}R_{\rm f} + i\vec{k}_{\rm f}\cdot\vec{R}_{\rm f}){\rm d}\vec{t}_1{\rm d}\vec{R}_{\rm f}{\rm d}x, \tag{10}$$

where $\vec{K}_s = \mu_b\vec{k}_{\rm i} - \vec{k}_{\rm f}$, $\vec{t}_1 = \vec{q} + (1-x)\vec{C}$, $\eta_1^2 = x(1-x)C^2 + S_n^2 x + (1-x)(\beta^2/\mu_a^2)$ and $\vec{C} = \mu_C\vec{k}_{\rm i}$.

Again applying the Fourier transform

$$\int \frac{\mathrm{e}^{i\vec{p}\cdot\vec{r}}}{(p^2+\lambda^2)^2} = \frac{\pi^2}{\lambda}\mathrm{e}^{-\lambda r} \tag{11}$$

eq. (10) takes the form

$$I = \frac{2\pi}{\mu_a^2}\int\int_0^1 \mathrm{e}^{-\eta_1 R_\mathrm{f} + i\vec{Q}\cdot\vec{R}_\mathrm{f}}{}_1F_1(-i\alpha;1;ik_\mathrm{f}R_\mathrm{f} + i\vec{k}_\mathrm{f}\cdot\vec{R}_\mathrm{f})\mathrm{d}\vec{R}_\mathrm{f}\frac{\mathrm{d}x}{\eta_1}, \tag{12}$$

where $\vec{Q} = \frac{\vec{k}_\mathrm{i}}{\mu_a} - \vec{k}_\mathrm{f} + \mu_C\vec{k}_\mathrm{i}$.

Equation (12) may easily be integrated by using Nordseik integral [15] of the type

$$\begin{aligned}\int \mathrm{e}^{-\lambda r + i\vec{q}\cdot\vec{r}}{}_1F_1(-i\alpha;1;ipr + i\vec{p}\cdot\vec{r})\mathrm{d}\vec{r} \\ = -2\pi\frac{\mathrm{d}}{\mathrm{d}\lambda}\left[\left(\frac{q^2+\lambda^2}{2}\right)^{-i\alpha-1}\left(\frac{q^2+\lambda^2}{2} + \vec{p}\cdot\vec{q} - i\lambda\right)^{i\alpha}\right]\end{aligned} \tag{13}$$

$$I = -\frac{4\pi^2}{\mu_a^2}\int_0^1 \frac{\mathrm{d}}{\mathrm{d}\eta_1}\left[\left(\frac{Q^2+\eta_1^2}{2}\right)^{-i\alpha-1}\left(\frac{Q^2+\eta_1^2}{2} + \vec{k}_\mathrm{f}\cdot\vec{Q} - i\eta_1 k_\mathrm{f}\right)^{i\alpha}\right]\frac{\mathrm{d}x}{\eta_1}. \tag{14}$$

Equation (14) is a one-dimensional integral which can be numerically solved by using the Gauss–Legendre quadrature method. We have used 32 Gaussian points by taking proper care of convergence. Since in heavy particle collisions, the scattering amplitudes are sharply peaked in the forward direction and the angular spread of the scattering angle θ, we have used z as our integration variable instead of θ to obtain the total cross-section, where z is related to θ by the following transformation:

$$k_\mathrm{i}^2(1-\cos\theta) = (1+z)/(1-z). \tag{15}$$

The integration over z from -1 to $+1$ has been numerically performed by using Gauss–Legendre quadrature method by taking proper care of convergence.

3. Results and discussions

We have reported here the differential and total cross-sections when proton collides with either lithium or sodium atoms. The hydrogen atoms thus formed are always considered in the 2s excited state. All the results for total cross-sections have been presented in tabular form and the differential cross-sections in the graphical form.

Our total cross-sections data for lithium and sodium atoms (as shown in table 1) have been compared with available theoretical predictions obtained by CDW [8] and OBK [11] approximations and with those of Basuchoudhury and Sural [9] which they obtained by impulse approximation.

Our results are found in reasonably good agreement with the above-mentioned theoretical results. In figures 1–4, we have presented our differential cross-section results for proton-lithium and proton-sodium collisions. We considered here the

Table 1. Total charge transfer cross-section for proton-lithium and proton-sodium collisions are given in units of πa_0^2 (the bracketed numbers denote the powers of ten by which each entry should be multiplied).

Incident proton energy (keV)	$H^+ + Li(2s) \rightarrow H(2s) + Li^+$			$H^+ + Na(3s) \rightarrow H(2s) + Na^+$	
	σ_{CPB}	σ_{CDW}	σ_{OBK}	σ_{CPB}	σ_{IP}
50	0.3596(−2)		0.65(0)	0.5269(−2)	0.116(−2)
100	0.6746(−3)		0.10(−2)	0.4912(−2)	0.827(−4)
150	0.1294(−3)		0.49(−2)	0.1827(−2)	0.241(−4)
200	0.3294(−4)	0.1048(−4)	0.28(−2)	0.5206(−3)	0.103(−4)
250	0.1327(−4)				
300	0.8489(−5)				
500	0.9828(−6)	0.5212(−6)		0.6022(−6)	0.291(−6)
800	0.2278(−6)	0.7711(−7)		0.1029(−6)	
1000	0.9366(−7)	0.2906(−7)		0.1105(−7)	
2000	0.1079(−8)	0.1122(−10)		0.7331(−10)	
5000	0.5069(−11)	0.1032(−10)		0.1593(−11)	
8000	0.3234(−12)	0.8230(−12)		0.5387(−12)	
10,000	0.7195(−13)	0.2423(−12)		0.2088(−12)	

$\sigma_{CPB} \rightarrow$ Total cross-section in Coulomb projected Born approximation; $\sigma_{CDW} \rightarrow$ Total cross-section in continuum distorted wave approximation; $\sigma_{OBK} \rightarrow$ Total cross-section in OBK approximation by Ferrante *et al* [11]; $\sigma_{IP} \rightarrow$ Total cross-section in impulse approximation by Basuchoudhury and Sural.

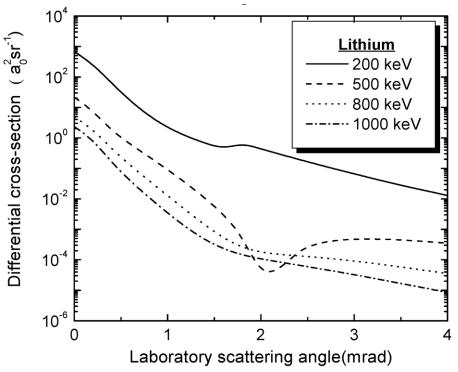

Figure 1. Differential cross-section (laboratory system) for $H^+ + Li(2s) \rightarrow H(2s) + Li^+$.

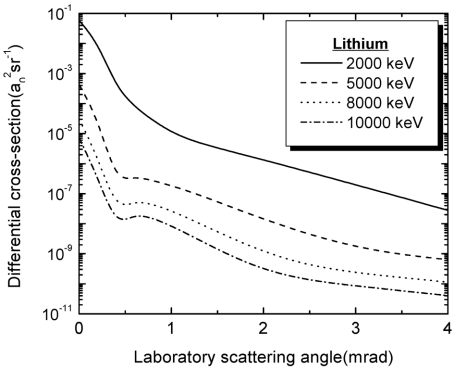

Figure 2. Differential cross-section (laboratory system) for $H^+ + Li(2s) \rightarrow H(2s) + Li^+$.

incident energies from 200 to 10,000 keV, for different scattering angles ranging from forward to high angular distributions.

We notice that in figure 2, at the incident energy 500 keV, there is a pronounced dip at about 2 mrad scattering angle. At incident energies 800 and 1000 keV, the nature of the curves are identical having small dips at about 2 and 1.5 mrad scattering angles. For the incident energies 200 keV, the nature of the curve is simply monotonically decreasing with the increase in the scattering angles. In figures 1 and 2 at incident energies 5000, 8000 and 10,000 keV, the dips at about 0.2 mrad scattering angles are very interesting. At 200 keV the nature of the curve is simply monotonically decreasing with increase of scattering angles. Similarly in figures 3

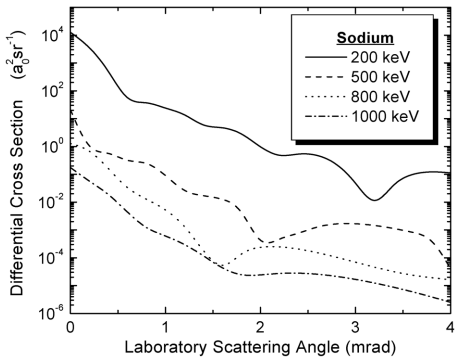

Figure 3. Differential cross-section (laboratory system) for H^++Na(3s) → H(2s) +Na^+.

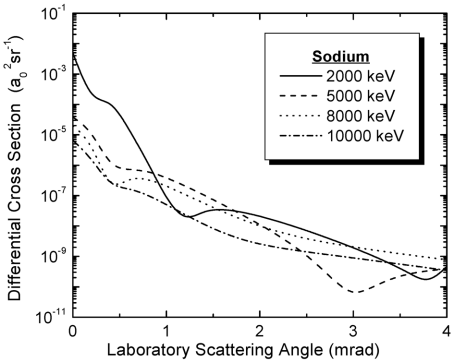

Figure 4. Differential cross-section (laboratory system) for H^++Na(3s) → H(2s) +Na^+.

and 4 differential cross-sections for proton-sodium are presented. At incident energies 500 and 800 keV, the nature of the curves are somewhat similar but the dips occurred at 1.4 and 2 mrad. At incident energy 1000 keV, the differential cross-section decreases monotonically having a slight tendency of dip at about 1.9 mrad and then decreasing continuously with increase of angles. Similarly, at incident energies 200 and 5000 keV the nature of the graph seems to be similar having dips at about 1.2 and 3 mrad. It is not possible to compare our differential cross-section values with others, as no such results are available at higher incident energies as far as we know. Further investigations are needed at higher incident energies.

References

[1] J de Vries, R Hoekstra, R Morgenstern and T Schlatholter, *Phys. Rev. Lett.* **91**, 053401 (2003)
[2] T Schlatholter, R Hoekstra and R Morgenstern, *Int. J. Mass Spec.* **233**, 173 (2004)
[3] F Alvarado, S Bari, R Hoekstra and T Schlatholter, *Phys. Chem. Chem. Phys.* **8**, 1922 (2006)
[4] D Basu, S C Mukherjee and D P Sural, *Phys. Rep.* **42**, 145 (1978)
[5] Dz Belkic, R Gayet and A Salin, *Phys. Rep.* **56**, 279 (1979)
[6] R K Janev and L P Presenyakov, *Phys. Rep.* **70**, 1 (1981)
[7] B H Bransden and R K Janev, *Adv. At. Mol. Phys.* **19**, 1 (1983)
[8] K E Banyard and G W Shirtclliffe, *J. Phys.* **B12**, 18 3247 (1979)
[9] K Basuchoudhury and D P Sural, *J. Phys.* **B25**, 853 (1992)
[10] S Geltman, *J. Phys.* **B4**, 1288 (1971)
[11] G Ferrante, E Fiordillino and M Zarcone, *Nuovo Cimento* **B52**, 151 (1979)
[12] M R C McDowell and J P Coleman, *Introduction to the theory of ion-atom collisions* (North-Holland, Amsterdam, 1970) p. 364
[13] P Simsic and W Williamson Jr, *Chem. Phys.* **57**, 323 (1972)
[14] R P Feynman, *Phys. Rev.* **76**, 769 (1949)
[15] A Nordseik, *Phys. Rev.* **93**, 785 (1954)